

# A nonlinear interval-based optimization method with local-densifying approximation technique

Ziheng Zhao · Xu Han · Chao Jiang · Xingxing Zhou

Received: 23 December 2008 / Revised: 5 February 2010 / Accepted: 25 February 2010 / Published online: 14 April 2010  
© Springer-Verlag 2010

**Abstract** In this paper, a new method is proposed to promote the efficiency and accuracy of nonlinear interval-based programming (NIP) based on approximation models and a local-densifying method. In conventional NIP methods, searching for the response bounds of objective and constraints are required at each iteration step, which forms a nested optimization and leads to extremely low efficiency. In order to reduce the computational cost, approximation models based on radial basis functions (RBF) are used to replace the actual computational models. A local-densifying method is suggested to guarantee the accuracy of the approximation models by reconstructing them with densified samples in iterations. Thus, through a sequence of optimization processes, an optimal result with fine accuracy can be finally achieved. Two numerical examples are used to test the effectiveness of the present method, and it is then applied to a practical engineering problem.

**Keywords** Uncertain optimization · Nonlinear interval-based programming · Approximation model · Radial basis functions · Local-densifying

## 1 Introduction

Parameter uncertainty widely exists in engineering optimization problems. Typical uncertainties can be found in geometric dimensions, material properties, loads and

boundary conditions, etc. Various methods have been developed for design optimization under uncertainty based on probabilistic method known as reliability-based optimization or robust optimization, and works in this field include: first/second order reliability method (Zhao and Ono 1999), first order second moment (Jung and Lee 2002), adaptive importance sampling technique (Au and Beck 1999), advanced mean value (Wu et al. 1990) and its hybrid variant (Youn et al. 2003), sequential optimization and reliability assessment (Du and Chen 2004), and single-loop design method (Liang et al. 2004), etc. Lee and Chen (2009) conduct an in-depth examination of several widely used probabilistic techniques. In these methods, uncertain parameters are treated as random variables, and their precise probability distribution functions should be predefined based on a large amount of information. However, the fact is that the process of getting adequate uncertainty information is generally expensive and time-consuming, and sometimes even impossible. Additionally, the literature (Ben-Haim and Elishakoff 1990) has shown that small deviations of the parameter probability distributions from the real distributions may cause large errors. Therefore, for many engineering problems without enough uncertainty information, the probabilistic methods will encounter difficulty inevitably.

Different strategies have been studied to overcome the aforementioned limitations of the probabilistic models. For many practical design problems, the bounds of the uncertain parameters can be much more easily identified compared with creating the precise probability distributions. Thus, non-probabilistic models have been considered as attractive supplements to the conventional probabilistic models in practical engineering design problems (Möller and Beer 2008). The uncertain-but-bounded parameters can be treated as convex models such as ellipsoid and interval set (Ben-Haim and Elishakoff 1990). This concept of convex

Z. Zhao · X. Han (✉) · C. Jiang · X. Zhou  
State Key Laboratory of Advanced Design and Manufacturing  
for Vehicle Body, College of Mechanical and Vehicle Engineering,  
Hunan University, Changsha City, 410082,  
People's Republic of China  
e-mail: xu\_han688@hotmail.com, hanxu@hnu.cn

model has been applied to reliability-based design optimization (Ben-Haim 1994; Elishakoff 1995). Since then, optimization under uncertainty using interval models has been addressed by a number of studies, which include: interval arithmetic (Rao and Cao 2002), tolerance box (Parkinson 1995), multi-point approximation (Penmetsa and Grandhi 2002), anti-optimization (Lombardi and Haftka 1998), sensitivity region (Gunawan and Azarm 2005) and multi-ellipsoid convex model (Luo et al. 2008).

Interval models are applicable to problems with incomplete information. It considers only the lower and upper bounds of the uncertain parameters without assuming their precise probability distribution functions. For a specific design point, the responses of objective function and constraints construct intervals due to the interval uncertainty. The bounds of these intervals are the minimal and maximal responses of objective and constraints under the uncertainty. Combined with perturbation technique, interval mathematics was used by Qiu and Elishakoff (1998), Elishakoff et al. (1994) to treat uncertain-but-bounded parameters in the sizing optimization of truss structures. Jiang et al. (2007a) proposed an efficient nonlinear interval number programming method using interval analysis based on the Taylor expansion. These local expansion-based methods, such as Taylor series expansion and perturbation method are difficult to work well when the large variation of uncertain parameters and high nonlinearity of the system are involved. Recently, progresses (Ma 2002) have been made in NIP problem. Attempt has been done to integrate the probabilistic model and interval model together to describe the uncertainties in reliability based design (Du and Sudjianto 2005). Jiang et al. (2008) proposed a general NIP method in which not only the uncertain objective function but also the uncertain constraints are nonlinear, and the variation of the uncertain parameters can be relatively large. In that method, searching for minimal and maximal responses of the objective and constraints is integrated with the main optimization, thus a nested optimization is formed. Besides, most of practical design problems are based on time-consuming simulation models such as FEM, and hence such a nested optimization using actual simulation model will lead to extremely low efficiency.

How to quantify the uncertainty correctly is only one side of the problem, and how to solve the corresponding uncertain optimization efficiently seems a more important side of the problem (Beyer and Sendhoff 2007). Most of the current works focus on modeling the interval-based optimization problems, while this paper places emphasis on solving the NIP problem efficiently and accurately. Currently, approximation models are often used in the computationally intensive optimization problems, which can provide fast estimations of the objective and constraints at new design points. The NIP methods using approximation

techniques, named approximation nonlinear interval-based programming (ANIP), are capable to deal with complex engineering problems (Jiang et al. 2007b). The commonly used approximation techniques are: polynomial response surface methodology (Myers and Montgomery 2002), kriging (Sacks et al. 1989; Martin and Simpson 2005), neural networks (Smith 1993), radial basis function (Dyn et al. 1986; Mullur and Messac 2004) and support vector regression (Clarke et al. 2005). In general, there are no clear conclusions on which approximation model is superior among others for every problem (Jin 2005; Acar and Solanki 2009). In this work, RBF approximation model is used because of its fine performance on computational efficiency, numerical stability and capacity of capturing nonlinear behavior (Jin et al. 2001). The accuracy of the approximation is one of the most important issues in all kinds of approximation assisted optimization methods, but in ANIP methods, we only care about the accuracy of approximations in some local regions which have key effects on optimal results. However, design of experiment (DOE) methods such as Latin hypercube design and orthogonal design generate samples using uniform distributions in the entire sampled space. Consequently, if we want to obtain more precise approximations at the concerned regions, we have to increase sample size over the whole sampled space. In fact, the approximation requirement in unconcerned regions can be relaxed for the sake of saving computational cost.

To realize the abovementioned concept, a local-densifying method combined with RBF approximation model is proposed. In the local-densifying method, the current best combinations consisted of the current best design and its corresponding boundary uncertain parameters are sequentially added to the local regions where the minimal and maximal responses of current approximation models take place. Then the RBF approximation models are reconstructed using these densified samples for next iteration until the stop criteria are reached. From the view point of DOE techniques, this proposed local-densifying method is an adaptive DOE method or an on-line approximation method since the new design points are selected according to some specific criteria. However, most of the adaptive DOE methods are developed for deterministic optimization problems (Wang 2003; Li et al. 2007, 2008; Jin 2005). The research works on developing adaptive approximation optimization techniques for NIP is still sparse. In this paper, we attempt to address this topic.

The rest of this paper is organized as follows. A general NIP model is firstly given and the conventional ANIP method is introduced. A new ANIP method with local-densifying method based on RBF models is then proposed, which is the core of this paper. Finally, two numerical examples and a practical engineering application are provided to demonstrate the effectiveness of the present method.

### 2 Statement of the problem

A NIP problem is given as follows:

$$\min_{\mathbf{X}} f(\mathbf{X}, \mathbf{U})$$

subject to

$$\begin{aligned} g_i(\mathbf{X}, \mathbf{U}) &\leq_{mw} V_i^I = [V_i^L, V_i^R], \quad i = 1, \dots, l \\ \mathbf{U} \in \mathbf{U}^I &= [\mathbf{U}^L, \mathbf{U}^R], U_i \in U_i^I = [U_i^L, U_i^R], \quad i = 1, 2, \dots, q \\ \mathbf{X}_l &\leq \mathbf{X} \leq \mathbf{X}_r \end{aligned} \tag{1}$$

where  $\mathbf{X}$  is an  $n$ -dimensional design vector, and  $\mathbf{X}_l$  and  $\mathbf{X}_r$  denote the allowable lower and upper boundary vectors of  $\mathbf{X}$ , respectively.  $\mathbf{U}$  is a  $q$ -dimensional uncertain vector which contains all the uncertain parameters in the system and the uncertain interval vector  $\mathbf{U}^I$  denotes their uncertainty. The superscript  $I$  indicates an interval, and  $L$  and  $R$  denote the lower and upper bounds of the interval, respectively. Uncertainty space is defined as all  $\mathbf{U} \in \mathbb{R}^q$  that satisfy  $\mathbf{U}^L \leq \mathbf{U} \leq \mathbf{U}^R$ .  $V_i^I$  represents an allowable interval of the  $i$ th constraint.  $l$  is the number of the constraints.  $f$  and  $g_i$  represent the objective function and the  $i$ th constraint, respectively.  $f$  and  $g_i$  are usually obtained from the simulation models in practical applications. They are required to be both nonlinear functions of  $\mathbf{X}$  and  $\mathbf{U}$ , and continuous with respect to  $\mathbf{U}$  in our formulation. Note that the symbol  $\leq_{mw}$  represents that an interval is better than another but not that one is less than another (Ishibuchi and Tanaka 1990).

### 3 Treatment of the conventional ANIPs

Using the order relation in interval mathematics (Chanas and Kuchta 1996), the uncertain objective function can be transformed into two deterministic objective functions as follows (Ishibuchi and Tanaka 1990):

$$\min_{\mathbf{X}} [m(f(\mathbf{X}, \mathbf{U})), w(f(\mathbf{X}, \mathbf{U}))]$$

$$\begin{aligned} m(f(\mathbf{X}, \mathbf{U})) &= \frac{1}{2} (f^L(\mathbf{X}) + f^R(\mathbf{X})) \\ w(f(\mathbf{X}, \mathbf{U})) &= \frac{1}{2} (f^R(\mathbf{X}) - f^L(\mathbf{X})) \end{aligned} \tag{2}$$

where  $m(f(\mathbf{X}, \mathbf{U}))$  and  $w(f(\mathbf{X}, \mathbf{U}))$  are middle point and radius of the response interval of the objective function, respectively. For a specific design vector  $\mathbf{X}'$ , the possible values of  $f$  caused by the uncertainty will form an interval:

$$f(\mathbf{X}', \mathbf{U}) \in [f^L(\mathbf{X}'), f^R(\mathbf{X}')] \tag{3}$$

the lower bound and upper bound can be obtained using optimization methods:

$$f^L(\mathbf{X}') = \min_{\mathbf{U}} f(\mathbf{X}', \mathbf{U}), \quad f^R(\mathbf{X}') = \max_{\mathbf{U}} f(\mathbf{X}', \mathbf{U})$$

$$\mathbf{U}^L \leq \mathbf{U} \leq \mathbf{U}^R \tag{4}$$

Jiang proposed a modified satisfaction degree of interval number which represents a certain degree that one interval number is better (or worse) than another.

$$P(A_i^I \leq_{mw} B_i^I) \geq \lambda_i \quad (P, \lambda_i \in [0, 1])$$

$$A_i^I = g_i(\mathbf{X}, \mathbf{U}) = [g_i^L(\mathbf{X}), g_i^R(\mathbf{X})], \quad B_i^I = [v_i^L, v_i^R]$$

$$g^L(\mathbf{X}) = \min_{\mathbf{U}} g(\mathbf{X}, \mathbf{U}), \quad g^R(\mathbf{X}) = \max_{\mathbf{U}} g(\mathbf{X}, \mathbf{U}) \tag{5}$$

where the satisfaction degree  $P(A^I \leq_{mw} B^I)$  can be computed through the following formula (Jiang et al. 2008):

$$P(A^I \leq_{mw} B^I) = \begin{cases} 0, & A^L \geq B^R \\ 0.5 \cdot \frac{B^R - A^L}{A^R - A^L} \cdot \frac{B^R - A^L}{B^R - B^L}, & B^L \leq A^L < B^R \leq A^R \\ \frac{B^L - A^L}{A^R - A^L} + 0.5 \cdot \frac{B^R - B^L}{A^R - A^L}, & A^L < B^L < B^R \leq A^R \\ \frac{B^L - A^L}{A^R - A^L} + \frac{A^R - B^L}{A^R - A^L} \cdot \frac{B^R - A^R}{B^R - B^L}, & A^L < B^L \leq A^R < B^R \\ \quad + 0.5 \cdot \frac{A^R - B^L}{A^R - A^L} \cdot \frac{A^R - B^L}{B^R - B^L}, & \\ \frac{B^R - A^R}{B^R - B^L} + 0.5 \cdot \frac{A^R - A^L}{B^R - B^L}, & B^L \leq A^L < A^R < B^R \\ 1, & A^R < B^L \end{cases}$$

where  $A_i^I$  is the interval of the  $i$ th constraint at  $\mathbf{X}$  and  $B_i^I$  is the  $i$ th allowable interval.  $P$  represents the satisfaction degree that the constraint is satisfied.  $\lambda_i$  is a predetermined satisfaction level. The feasible field of the constraints (5) can be controlled by adjusting the value of  $\lambda_i$ , namely a greater  $\lambda_i$  indicates a smaller feasible field.

Linear combination method is then employed to integrate the deterministic two objective functions, and the penalty function method is used to deal with the constraints. Thus a single-objective optimization problem in terms of a penalty function is finally constructed:

$$\begin{aligned} \min_{\mathbf{X}} f_p &= (1 - \beta) \frac{(m(f(\mathbf{X}, \mathbf{U})) + \xi)}{\phi} \\ &+ \beta \frac{(w(f(\mathbf{X}, \mathbf{U})) + \xi)}{\psi} \\ &+ \sigma \sum_{i=1}^l \varphi(P(A_i \leq_{mw} B_i) - \lambda_i) \end{aligned}$$

Subject to

$$\mathbf{X}_l \leq \mathbf{X} \leq \mathbf{X}_r \tag{6}$$

where  $0 \leq \beta \leq 1$  is a weighting factor of the two objective functions.  $\xi$  is a number making  $m(f(\mathbf{X}, \mathbf{U})) + \xi$  and  $w(f(\mathbf{X}, \mathbf{U})) + \xi$  non-negative.  $\phi$  and  $\psi$  are two normalization factors.  $\sigma$  is a penalty factor which is usually specified as a large value.  $\varphi$  is a function in the following form:

$$\begin{aligned} &\varphi(P(A_i \leq_{mw} B_i) - \lambda_i) \\ &= \max[0, -(P(A_i \leq_{mw} B_i) - \lambda_i)]^2 \end{aligned} \tag{7}$$

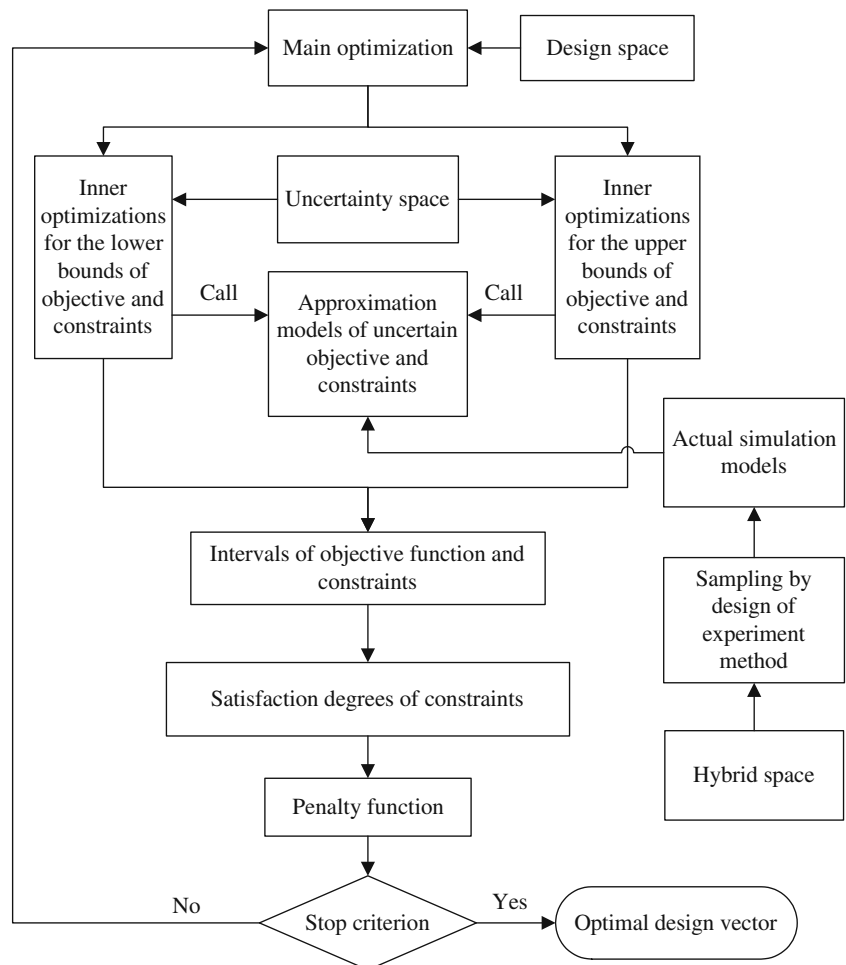
Equation 6 can be solved by traditional optimization methods. It can be found from (4) and (5) that the inner optimizations are involved in each main optimization step. The computational cost will be very expensive when the simulation models are time-consuming. Approximation models thus can be used to improve the computation efficiency, and

then the general NIP problem (1) can be transformed into the following ANIP problem:

$$\begin{aligned} &\min_{\mathbf{X}} \tilde{f}(\mathbf{X}, \mathbf{U}) \\ &\text{subject to} \\ &\tilde{g}_i(\mathbf{X}, \mathbf{U}) \leq_{mw} V_i^I = [V_i^L, V_i^R], \quad i = 1, \dots, l \\ &\mathbf{U} \in \mathbf{U}^I = [\mathbf{U}^L, \mathbf{U}^R], U_i \in U_i^I = [U_i^L, U_i^R], \quad i = 1, 2, \dots, q \\ &\mathbf{X}_l \leq \mathbf{X} \leq \mathbf{X}_r \end{aligned} \tag{8}$$

where  $\tilde{f}$  and  $\tilde{g}_i$  represent the approximate objective function and constraints, respectively. A conventional solving process for the ANIP optimization can be outlined in Fig. 1. At each iteration, uncertain parameters are treated the same as design variables, thus a  $n + q$  dimensional hybrid space is formed. DOE methods are used to select the samples within the hybrid space. Then the approximation models can be built using these samples. Consequently, the computational efficiency can be greatly improved, but the accuracy

**Fig. 1** Optimization process of a NIP problem based on approximation models



of the optimal results obtained by ANIP methods cannot be guaranteed through this one-step approximation.

#### 4 Local-densifying method based on RBF approximation models

##### 4.1 Radial basis functions approximation

Radial basis functions have been developed for the interpolation of scattered multivariate data (Queipo et al. 2005). The method uses linear combinations of radially symmetric functions based on Euclidean distance or other such metric. A RBF model can be expressed as:

$$\tilde{f}(\mathbf{x}_p) = \sum_i^m w_i h_p(r_i) \tag{9}$$

where  $w_i$  represents the coefficient of the linear combinations.  $m$  is the number of samples.  $\mathbf{x}_p$  represents the vector of estimation point  $p$ .  $h_p(r_i)$  is the radial basis function with respect to the Euclidean distance between the estimation point  $p$  and  $i$ th sample where  $r_i = \|\mathbf{x}_p - \mathbf{x}_i\|_2$ . The main feature of radial basis functions is that their response decreases or increases monotonically with the variable  $r$ . Some commonly used radial basis functions are multi-quadratics, thin plate spline and Gaussian. In our work, the Gaussian radial basis function is adopted:

$$h_p(r_i) = \exp\left(-r_i^2/c^2\right) \tag{10}$$

The parameter  $c$  is the average spacing of all the samples. It controls the decay rate of the function. A set of  $m$  samples are needed to define the coefficients of RBF model which can be expressed in matrix form as:

$$\mathbf{f} = \mathbf{H}\mathbf{w} \tag{11}$$

where  $\mathbf{H}$  is a matrix:

$$\mathbf{H} = \begin{pmatrix} h_1(r_1) & h_1(r_2) & \cdots & h_1(r_m) \\ h_2(r_1) & h_2(r_2) & \cdots & h_2(r_m) \\ \vdots & \vdots & \ddots & \vdots \\ h_m(r_1) & h_m(r_2) & \cdots & h_m(r_m) \end{pmatrix} \tag{12}$$

If the inverse of  $\mathbf{H}$  exists, the coefficient vector can be obtained:

$$\mathbf{w} = \mathbf{H}^{-1}\mathbf{f} \tag{13}$$

It has been proved that the matrix  $\mathbf{H}$  is always invertible for arbitrary scattered samples (Liu 2003).

In conventional ANIP method, large approximate errors in the bounds of response intervals will make the results untrustworthy. To improve the precision, a large sample size is needed to construct high-fidelity approximation models. There is a trade-off between accuracy and efficiency. To pursue high efficiency, sometimes we have to sacrifice the high accuracy. In conventional ANIP methods, the samples are uniformly selected by DOE methods. It is necessary to arrange the samples more appropriately because the result of NIP method is only significantly affected by some key local regions.

##### 4.2 Iterative mechanism

Local-densifying method is an updating strategy of sampling method focusing the limited sample resources on the concerned local regions. The RBF approximation models are reconstructed using the local densified samples in each iteration step. Therefore, it ensures that the approximations have small approximate errors on the bounds of response intervals so that the result can be more reliable. However, local-densifying may lead to overlap of some samples, and thus the matrix  $\mathbf{H}$  would be singular or ill-conditioned. Therefore, a treatment is needed to exclude the added points which are too close to the previous samples.

The iterative process of local-densifying method based on RBF approximation models for ANIP is outlined as follows:

- (a) Obtain initial samples by Latin hypercube design method within the hybrid space, and give allowable errors  $\varepsilon_1 > 0$  and  $\varepsilon_2 > 0$ , and make  $j = 1$ .
- (b) Create RBF approximation models with the samples, and construct the ANIP problem by replacing the objective function and constraints with the approximation models. Then, the current best design vector  $\mathbf{X}^{(j)}$  is obtained by solving the ANIP problem.
- (c) The response interval  $[\tilde{f}^L(\mathbf{X}^{(j)}), \tilde{f}^R(\mathbf{X}^{(j)})]$  of approximate objective and corresponding uncertain parameters  $\mathbf{U}_f^L$  and  $\mathbf{U}_f^R$  can be obtained:

$$\begin{aligned} \tilde{f}^L(\mathbf{X}^{(j)}) &= \tilde{f}(\mathbf{X}^{(j)}, \mathbf{U}_f^L), \\ \tilde{f}^R(\mathbf{X}^{(j)}) &= \tilde{f}(\mathbf{X}^{(j)}, \mathbf{U}_f^R) \end{aligned} \tag{14}$$

That means the approximate objective function achieves the minimum and maximum at the combinations  $(\mathbf{X}^{(j)}, \mathbf{U}_f^L)$  and  $(\mathbf{X}^{(j)}, \mathbf{U}_f^R)$ , respectively. Similarly, the response intervals of the approximate constraints  $[\tilde{g}_z^L(\mathbf{X}^{(j)}), \tilde{g}_z^R(\mathbf{X}^{(j)})], z = 1 \cdots l$  and cor-

responding uncertain parameters  $\mathbf{U}_{g_z}^L, \mathbf{U}_{g_z}^R, z = 1 \dots l$  are obtained:

$$\begin{aligned} \tilde{g}_z^L(\mathbf{X}^{(j)}) &= \tilde{g}_z(\mathbf{X}^{(j)}, \mathbf{U}_{g_z}^L), \\ \tilde{g}_z^R(\mathbf{X}^{(j)}) &= \tilde{g}_z(\mathbf{X}^{(j)}, \mathbf{U}_{g_z}^R), z = 1 \dots l. \end{aligned} \tag{15}$$

The  $z$ th approximate constraint achieves the lower and upper bounds at the combinations  $(\mathbf{X}^{(j)}, \mathbf{U}_{g_z}^L)$  and  $(\mathbf{X}^{(j)}, \mathbf{U}_{g_z}^R)$ , respectively.

- (d) Compute the responses of actual objective  $[f^L(\mathbf{X}^{(j)}), f^R(\mathbf{X}^{(j)})]$  and actual constraint  $[g_z^L(\mathbf{X}^{(j)}), g_z^R(\mathbf{X}^{(j)})]$ ,  $z = 1 \dots l$  at the combinations obtained from step (c).

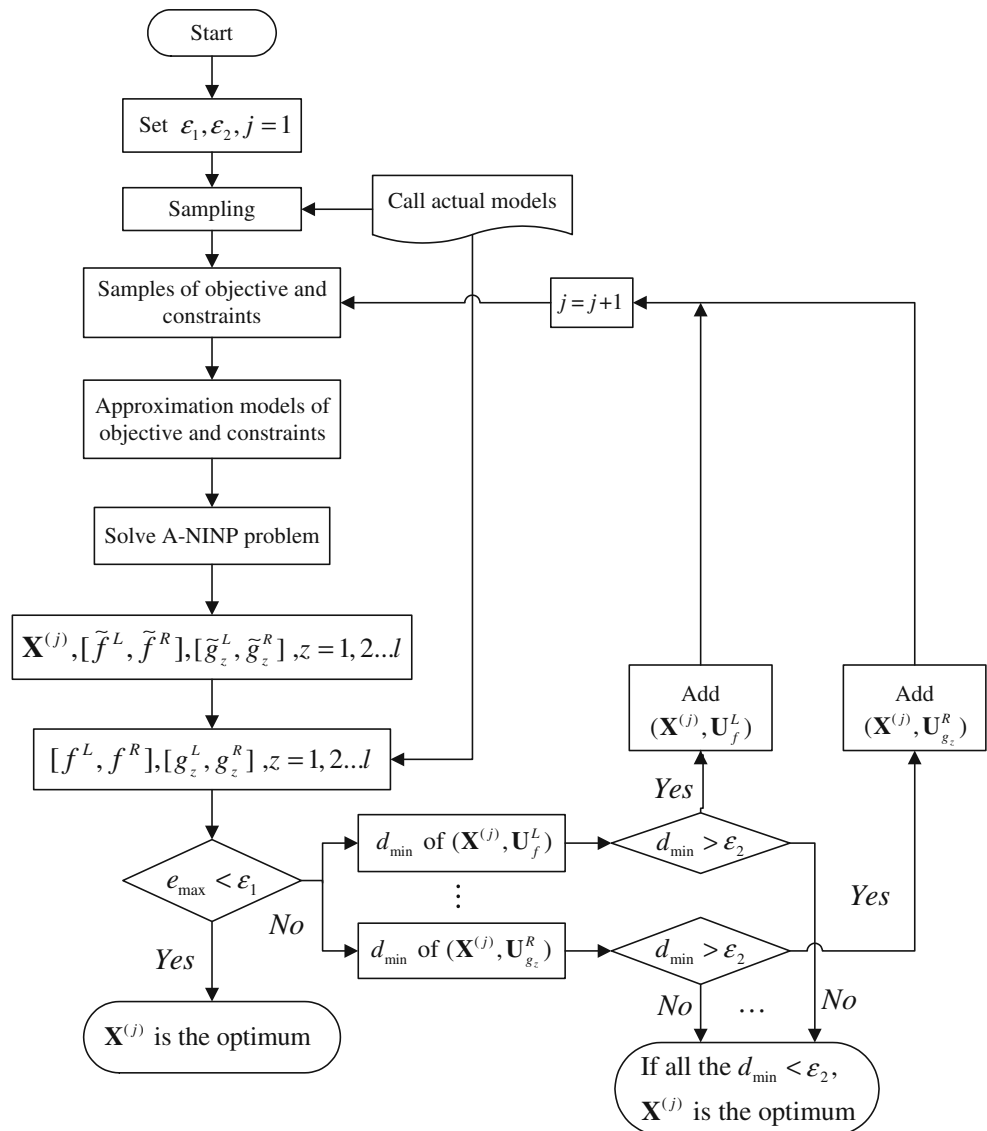
- (e) Compute the deviation  $e_{\max}$ :

$$e_{\max} = \max \left\{ \left| \frac{f^L - \tilde{f}^L}{f^L} \right| + \left| \frac{f^R - \tilde{f}^R}{f^R} \right|, \left| \frac{g_z^L - \tilde{g}_z^L}{g_z^L} \right| + \left| \frac{g_z^R - \tilde{g}_z^R}{g_z^R} \right|, z = 1 \dots l \right\} \tag{16}$$

If  $e_{\max} < \varepsilon_1$ , then  $\mathbf{X}^{(j)}$  is selected as the final optimal design vector and the iteration terminates, otherwise, turn to step (f).

- (f) Calculate the distances between  $(\mathbf{X}^{(j)}, \mathbf{U}_f^L)$  and all the other samples and obtain the minimal distance  $d_{\min}$ . If  $d_{\min} > \varepsilon_2$ , add  $(\mathbf{X}^{(j)}, \mathbf{U}_f^L)$  to the sample set; calculate the distances between the combination  $(\mathbf{X}^{(j)}, \mathbf{U}_f^R)$  and all the samples and obtain the minimal distance  $d_{\min}$ . If

**Fig. 2** Uncertain optimization method combined A-NIP with local-densifying method



$d_{\min} > \varepsilon_2$ , then add  $(\mathbf{X}^{(j)}, \mathbf{U}_f^R)$  to the samples. Similarly, the boundary combinations of each constraint are all treated with the above process, and the combinations, which do not satisfy  $d_{\min} > \varepsilon_2$ , are excluded. If all the boundary combinations fail to satisfy  $d_{\min} > \varepsilon_2$ , the iteration terminates, and  $\mathbf{X}^{(j)}$  is selected as the final optimal design vector; otherwise, set  $j = j + 1$  and turn to step (b).

In step (a), the initial sample size can be relatively small because the initial approximation models, which are used as guides for the subsequent densifying, do not need to be highly accurate. The aim of this step is to construct approximation models capturing the major characteristics of the actual objective function and constraints. They can help to identify the regions that should be densified. However, the sample size can not be too small. A too small sample size may result in the loss of key information. For such case, the optimization may converge to the local optimum. In step (c), the main optimization and the inner optimizations are both solved by intergeneration projection genetic algorithm (IP-GA; Xu et al. 2001), which is a modification based on micro GA (Krishnakumar 1989).

In step (e), the stop criterion  $e_{\max} < \varepsilon_1$  is used, whose satisfaction indicates that the approximation models of objective and constraints have a fine approximate accuracy at the neighborhoods of the lower and upper bounds. That can ensure the trustworthiness of the optimal result, since the computation of ANIP method greatly depends on these response bounds.

Step (f) is the process of sample densifying. Current best combinations are added to the samples at each iteration step, and then the approximation accuracy in the boundary regions can be improved gradually. From (12), we can find that if two samples overlap or locate too close, the  $\mathbf{H}$  matrix will be singular or ill-conditioned and the RBF approximation models will fail to be constructed. Additionally, we can see from the decreasing feature of Gaussian radial function that the estimations within the neighborhood of a sample have high approximate accuracy. In other words, it does not help to promote the approximate accuracy when the distance between two samples becomes very close. They will, in contrast, make the computation unstable. Therefore, an allowable error  $\varepsilon_2$  is set to determine which boundary combinations should be excluded. A high approximate accuracy in the key regions are considered to be attained when all the boundary points satisfy the condition  $d_{\min} < \varepsilon_2$ , and then the iteration terminates.

The flowchart of the present method is shown in Fig. 2. It can be found that the computation time is spent in three parts. The first part is to compute the samples for constructing the approximation models. For complex simulation models, it would dominate the process. The second one is

to search the bounds of objective and constraints. As the approximation models are used, the optimization efficiency can be very high. The third one is to validate the approximation responses, in which the actual responses of the objective and constraints need to be computed.

### 5 Numerical examples and discussions

Two numerical examples are given to test the proposed method. The first simply numerical test is given for the purpose of intuitively understanding how this method processes. The second complex numerical test is present to compare the proposed method with the conventional method with respect to the computational efficiency and accuracy. Finally, a practical engineering application is provided to demonstrate the effectiveness of the present method in real-world engineering.

#### 5.1 Numerical test 1

A numerical test problem is given as:

$$\begin{aligned} & \min_x f(x, u) \\ & = -24 \sin \left( \sqrt{\left(\frac{x-40}{2}\right)^2 + (u-5)^2} \right) / \\ & \quad \sqrt{\left(\frac{x-40}{2}\right)^2 + (u-5)^2} + 46 \end{aligned}$$

subject to

$$\begin{aligned} & 24 \leq x \leq 43 \\ & u \in U^I = [3.5, 16.5] \end{aligned} \tag{17}$$

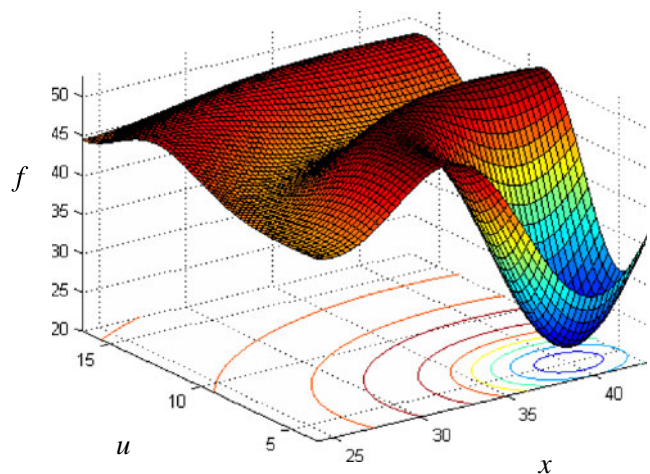


Fig. 3 Actual response of test function 1

**Table 1** Results with different initial sample number (test function 1)

ISN	$x^*$	$[f^L, f^R]$	$u^L, u^R$	$f_p$	NI	Nobj
5	24.00	[43.03, 48.19]	4.96, 12.41	5.67	8	21
10	39.99	[22.00, 51.20]	4.99, 9.57	5.56	13	36
20	40.03	[22.01, 51.21]	4.95, 9.50	5.56	8	36
30	39.92	[22.01, 51.21]	5.03, 9.49	5.56	2	34

This is a simple unidimensional optimization problem. The uncertainty level is given as a relatively large value  $\pm 65\%$  off from the midpoint. The normalization factors  $\phi$  and  $\psi$  are set to 5.0, respectively. The weighting factor  $\beta$  is specified as 0.4.  $\xi$  and  $\sigma$  are set to 0.0 and 100,000, respectively. The allowable errors  $\varepsilon_1$  and  $\varepsilon_2$  are set to 0.003 and 0.15, respectively. The number of objective function evaluations is used to examine the efficiency of this method.

Additionally, the actual response of the objective function is showed in Fig. 3. The optimal design variable 39.99 is obtained from the NIP method with the actual model, in which IP-GA is employed to solve the nested optimization. The maximal generations for IP-GA are both specified as 100. The optimal interval of objective function is [22.00, 51.21], and the corresponding boundary combinations are (39.99, 5.00) and (39.99, 9.50), respectively. The value of penalty function is 5.562. This result is used as an accurate solution to test the accuracy of the present method.

Four cases with 4 different initial sample sizes are investigated, and the optimization results are listed in Table 1, where ISN stands for the initial sample size, and  $x^*$  is the optimal design value. NI and Nobj stand for the total number of iterations and the number of objective function evaluations, respectively.

It can be found from Table 1 that the results obtained from the present method are almost the same as the accurate solution when the initial sample sizes are 10, 20 and 30. We can also see that the total number of iterations decreases as the number of initial samples increases. It needs only two iterations when the initial sample size is 30, which implies that 30 initial samples are sufficient to construct a high quality approximation model for this simple problem and there is no need to densify more samples. In the

fourth case, the number of objective function evaluations is less than the second and third cases even though the largest initial sample size is used. The results indicate that blindly decreasing the initial sample size would not help to reduce the computational cost, since fewer initial samples may lose the key information of the objective function. In the first case, five initial samples are used and the optimization process converges after eight iterations. The optimal design point is far from the accurate solution. The penalty function value, however, is very close to the accurate one. Two reasons lead to this result: Firstly, the NIP problem is solved by transforming the single-objective uncertain problem into two-objective deterministic problem. One objective minimizes the midpoint of the response interval and another minimizes the radius of the response interval. In such case, either the design point that causes the minimal midpoint or the one causes the minimal radius could be the optimal design. Secondly, if the key characteristics of the objective function are missed because of insufficiency of initial samples, the optimization will be hard to find the global optimum, and the local-densifying method is also difficult to refine the approximation model.

In order to interpret the details of this process better, Table 2 lists each iterative results of the third case. From the table, we can see that the approximate response interval  $[\tilde{f}^L, \tilde{f}^R]$  is far from the accurate response interval  $[f^L, f^R]$  under the same design variable at the beginning. The difference of  $[\tilde{f}^L, \tilde{f}^R]$  and  $[f^L, f^R]$  is getting smaller and smaller as the iteration proceeds. It shows that the initial approximation model has a globally low accuracy, and approximations in the boundary regions could achieve a high accuracy after several local-densifying steps. Figure 4 shows the transformation of the approximation model. The

**Table 2** Optimization results of the third case

Iteration	$x^*$	$u^L, u^R$	$[\tilde{f}^L, \tilde{f}^R]$	$[f^L, f^R]$
1	39.14	3.50, 16.50	[20.63, 50.28]	[30.63, 47.82]
2	38.06	4.62, 9.59	[26.49, 50.20]	[26.12, 51.12]
3	43.00	5.61, 11.46	[21.33, 49.25]	[31.19, 44.78]
4	42.65	5.00, 16.50	[29.08, 47.69]	[28.42, 47.73]
5	42.89	4.94, 9.61	[29.49, 48.74]	[29.53, 50.93]
6	40.86	4.97, 9.85	[23.23, 50.94]	[22.74, 50.86]
7	40.33	4.91, 9.61	[22.13, 51.07]	[22.14, 51.18]
8	40.03	4.95, 9.50	[22.04, 51.21]	[22.01, 51.21]



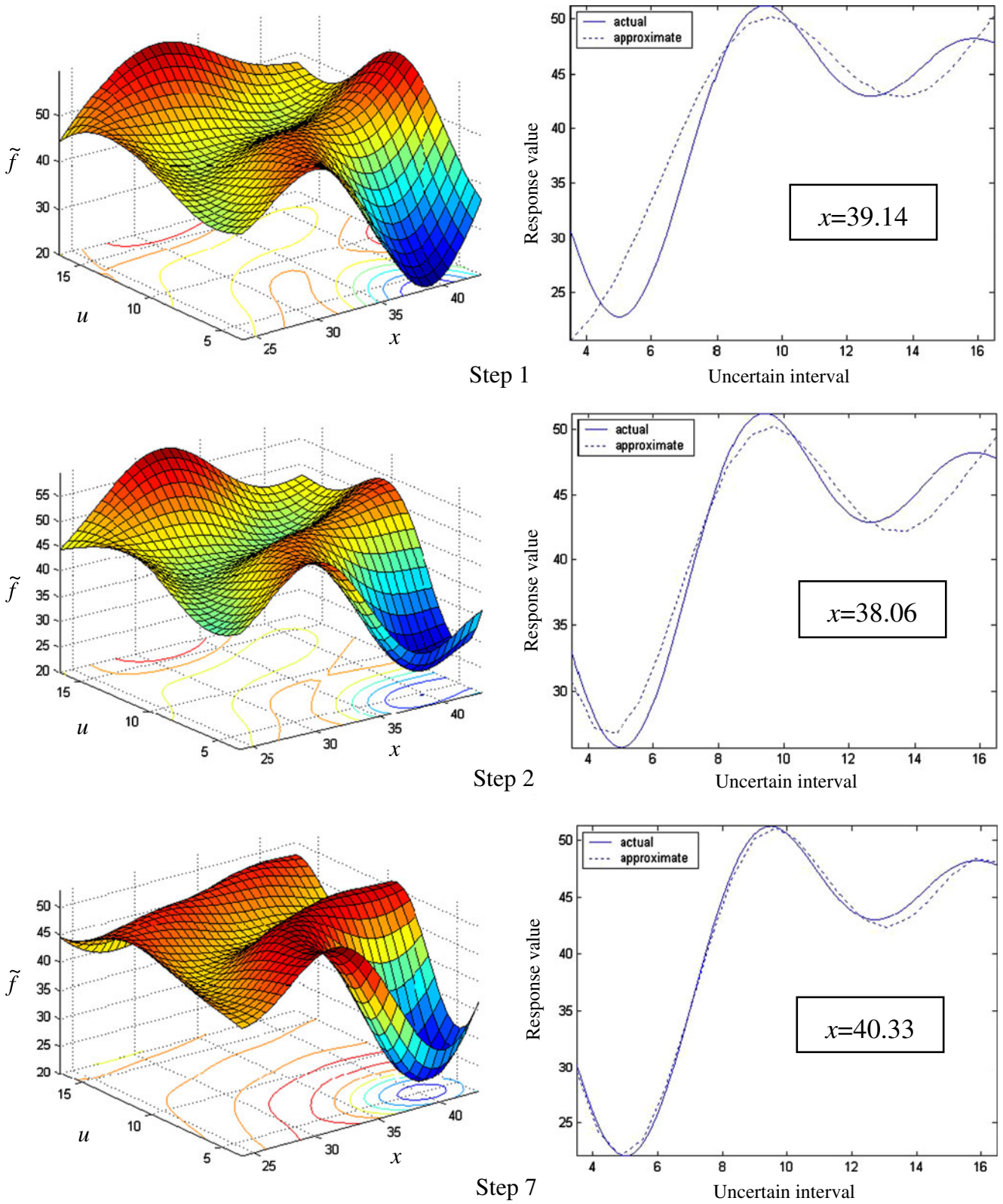


Fig. 4 Approximation models and section comparisons

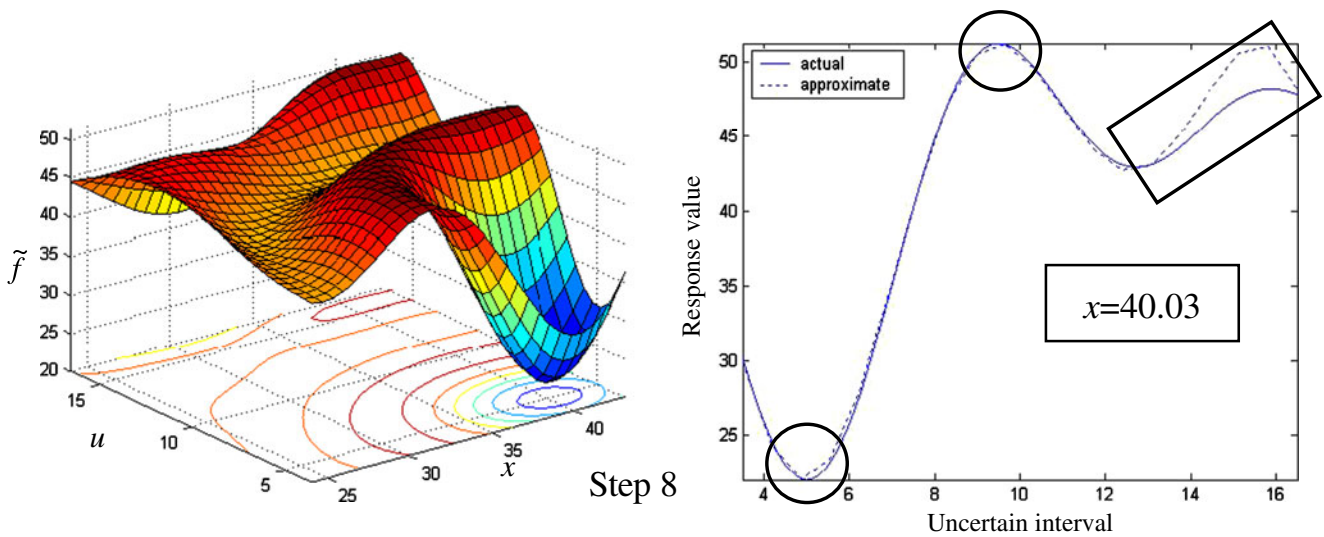


Fig. 4 (continued)

section curves of approximation model and actual model under the current best design in each iteration step can be compared visually.

We can learn from Fig. 4 that the section curves of approximation model and actual model are prone to coincidence on the lower and upper bounds as the iteration processes. At the final step, the two curves nearly overlap in the key regions marked with circles. As the lower and upper bounds of objective are only needed for the transformation of the uncertain optimization problem in (2), the poor approximation accuracy in the region marked with rectangle does not affect the optimal result. This feature shows

the advantage of local-densifying method that focuses the approximation accuracy only on the key regions and alleviates the requirement of approximation in the rest space. The distributions of samples at initial step and final step are shown in Fig. 5. We can see that the added points are densified in the local regions marked with circles, where the function has minimal and maximal responses under the optimal design variable, namely the neighborhoods of combinations (39.99, 5.00) and (39.99, 9.50). If the conventional ANIP method is used, the entire space should have the same sample density as these two local regions for constructing a high quality approximation model.

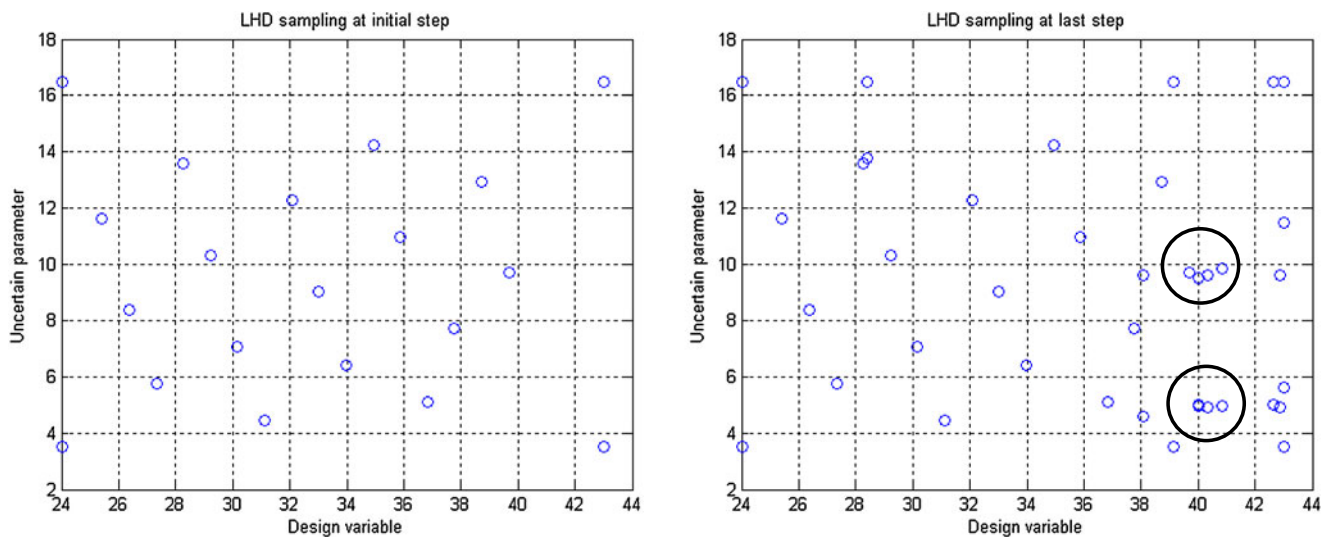


Fig. 5 Sample distributions of initial and last steps

**Table 3** Results of different initial sample numbers (test function 2)

ISN	Optimal design vector $\mathbf{X}^*$	Objective $[f^L, f^R]$	Constraint 1 $[g_1^L, g_1^R]$	Constraint 2 $[g_2^L, g_2^R]$	Satisfaction degree	$f_p$	NI	Nobj
30	(4.01, 0.57, -3.00)	[-3.47, 5.71]	[2.35, 26.43]	[7.50, 44.96]	0.82, 0.87	3.98	21	72
40	(4.07, 0.76, -2.78)	[-2.94, 5.65]	[2.64, 24.75]	[6.61, 40.49]	0.81, 0.83	3.99	20	80
50	(4.01, 0.63, -3.00)	[-3.49, 5.51]	[2.20, 24.72]	[6.96, 43.93]	0.80, 0.85	3.92	19	88
60	(4.02, 0.48, -3.00)	[-3.35, 5.95]	[2.61, 22.78]	[6.89, 43.46]	0.80, 0.85	4.03	16	92

5.2 Numerical test 2

A more complex three-dimensional testing problem with two inequality constraints is given as follows:

$$\min_{\mathbf{X}} f(\mathbf{X}, \mathbf{U}) = U_1 (X_1 - 2)^2 + U_2 (X_2 - 1)^2 + U_3 X_3$$

subject to

$$\begin{aligned} U_1 X_1^2 - U_2^2 X_2 + U_3 X_3 &\geq_{mw} [6.5, 7.0] \\ U_1 X_1 + U_2 X_2 + U_3^2 X_3^2 + 1 &\geq_{mw} [10.0, 15.0] \\ -2 \leq X_1 \leq 6, -4 \leq X_2 \leq 7, -3 \leq X_3 \leq 8 \\ U_1 \in [0.6, 1.8], U_2 \in [0.5, 1.5], U_3 \in [0.6, 2.0] \end{aligned} \quad (18)$$

$\mathbf{X}$  is the design variable vector and  $\mathbf{U}$  represents the uncertain parameter vector. The uncertainty level are given to relatively large values of 50%, 50% and 53.8%, respectively. The normalization factors  $\phi$  and  $\psi$  are set to 1.4 and 2.0 respectively. The weighting factor  $\beta$  is specified as 0.5.  $\xi$  and  $\sigma$  are set to 4.0 and 100000, respectively. The satisfaction levels of the two constraints  $\lambda_1$  and  $\lambda_2$  are both specified as 0.8. The allowable errors  $\varepsilon_1$  and  $\varepsilon_2$  are set to 0.05 and 0.15, respectively. The approximation models of

objective and constraints are built simultaneously, and the present method is applied.

Firstly, the accurate solution  $\mathbf{X} = (4.01, 0.87, -3.00)^T$  is obtained from the NIP method with actual models, in which IP-GA is employed to solve the nested optimization. The maximal number of generations for outer IP-GA is specified as 1,000 and the inner is specified as 300. The optimal response interval of objective function is [-3.49, 5.49]. The value of penalty function is 3.91.

Four cases with different initial sample sizes are investigated. The initial sample sizes are 30, 40, 50 and 60, and the results are listed in Table 3. As the initial sample size increases, the total iterations decrease gradually and the number of objective evaluations tends to increase. All the satisfaction degree at the optimal design points are satisfied (great than or equal to the satisfaction levels  $\lambda_1 = 0.8$  and  $\lambda_2 = 0.8$ ). Besides, the optimal results of the four cases slightly differ from the accurate solution  $\mathbf{X} = (4.01, 0.87, -3.00)^T$ , though all the penalty function values are close to the accurate one  $f_p = 3.91$ . It means that almost the same objective value is achieved with different optimal design variables, and all of them are acceptable for optimal design.

In the above four cases, the total numbers of the samples are 70, 78, 86 and 90, respectively. The conventional

**Table 4** Results of uniform distributional samples (test function 2)

Sample number	Optimal design	$[\tilde{f}^L, \tilde{f}^R] [\tilde{g}_z^L, \tilde{g}_z^R], z = 1, 2$	$[f^L, f^R] [g_z^L, g_z^R], z = 1, 2$	Satisfaction degree	$\tilde{f}_p$	$f_p$
70	(2.69, 0.42, 8.00)	[-6.02, 24.98] [0.86, 30.50] [6.94, 231.80]	[5.26, 17.37] [8.20, 28.94] [25.87, 262.47]	1.00, 1.00	9.69	7.98
78	(2.53, 0.68, 8.00)	[-9.96, 24.81] [1.83, 27.92] [7.66, 246.91]	[5.02, 16.66] [7.11, 27.33] [25.90, 262.57]	1.00, 1.00	9.43	7.75
86	(2.48, 0.44, 8.00)	[-8.57, 24.76] [1.49, 27.81] [5.11, 236.17]	[5.10, 16.89] [7.50, 26.97] [25.75, 262.13]	1.00, 1.00	9.48	7.83
90	(2.50, 0.69, 8.00)	[-7.25, 23.95] [2.05, 27.67] [7.65, 248.98]	[5.00, 16.60] [7.01, 27.12] [25.89, 262.54]	1.00, 1.00	9.31	7.74

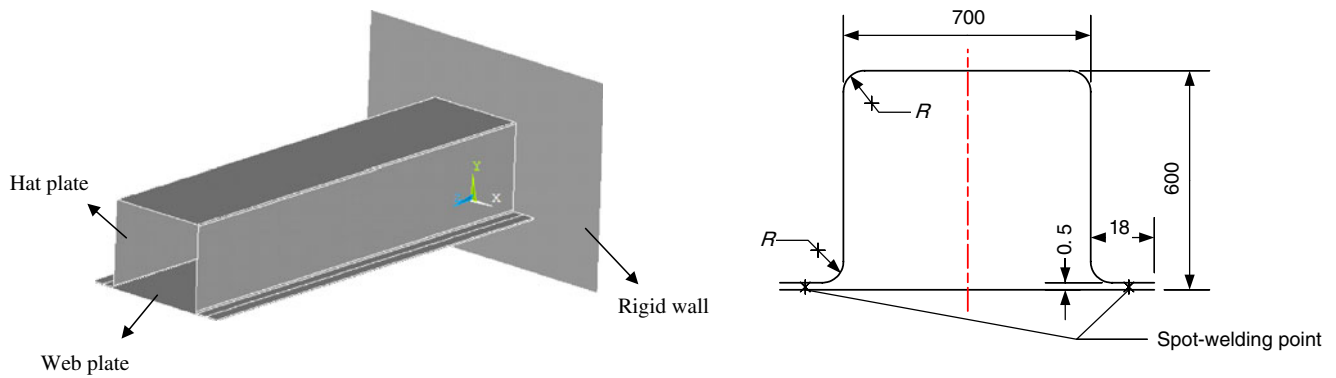


**Fig. 6** A closed-hat beam impacting the rigid wall and its cross-section (millimeter)

ANIP method is applied to solve this problem with the same sample size as the four cases finally use. The samples are distributed uniformly in the entire hybrid space by Latin hypercube design method. The outer and inner optimizations are both solved by IP-GA algorithm, and Table 4 lists the results. We can see that the errors on the bounds of response intervals between the approximation models and the actual models are large. In addition, the penalty function values at the optimal design are 7.98, 7.75, 7.83 and 7.74, while the optimal values are 3.98, 3.99, 3.92 and 4.03 in Table 3. It demonstrates the effectiveness of the present method and also indicates that a much more reliable and accurate result could be found with the same sample size compared to the conventional ANIP method. In such a six dimensional hybrid space, high accuracy approximation models are very difficult to be constructed by using limited samples with uniform distribution; nevertheless a fine result can be obtained by supplementing with local-densifying method.

### 5.3 Application for structural crashworthiness

An automobile thin-walled beam model as shown in Fig. 6 is investigated. Closed-hat beam, a typical thin-walled beam, is constructed by a hat-shaped part and a plate, connected by spot welds. It is one of the important structures of a vehicle body for load-support and energy-absorption for crashworthiness. Optimizing the thin-walled beam structures to improve their crashworthiness performance is very important to the vehicle security design. The application of structural optimization for a closed-hat beam impacting a rigid wall is investigated. Based on the reference (Kurtaran et al. 2002), the closed-hat beam will be optimized to maximize the absorbed energy subjected to an average normal impact force on the rigid wall. The research (Wang 2002) indicated that the plate thickness  $t$ , round radius  $R$  of the hat beam, and the space length  $d$  of each two neighboring

spot-welding points have prominent effects on the crashworthiness performance of a closed-hat beam, and hence these three parameters are used as design variables in this application.

The FEM model of the closed-hat beam impacting a rigid wall with the initial velocity of 10 m/s is shown in Fig. 7. The simulation duration of the impact process is set as 20 ms. An elasto-plasticity material model of bilinear kinematic hardening is used for the closed-hat beam, as given in Table 5.

The Belytschko–Tsay shell element is used to generate the FEM mesh, and the total number of the elements is 4,200. In order to achieve enough impact energy, a 250-kg mass is attached to the end of the closed-hat beam. The nominal values of the yield stress  $\sigma_s$  and tangent modulus  $E_t$  are 310 and 763 Mpa, respectively.  $\sigma_s$  and  $E_t$  are treated as the uncertain parameters because of the manufacturing and measuring errors. The uncertain level is 5% off from the normal values, namely  $\sigma_s \in [294.5 \text{ Mpa}, 325.5 \text{ Mpa}]$  and  $E_t \in [724.85 \text{ Mpa}, 801.15 \text{ Mpa}]$ . As a result, this

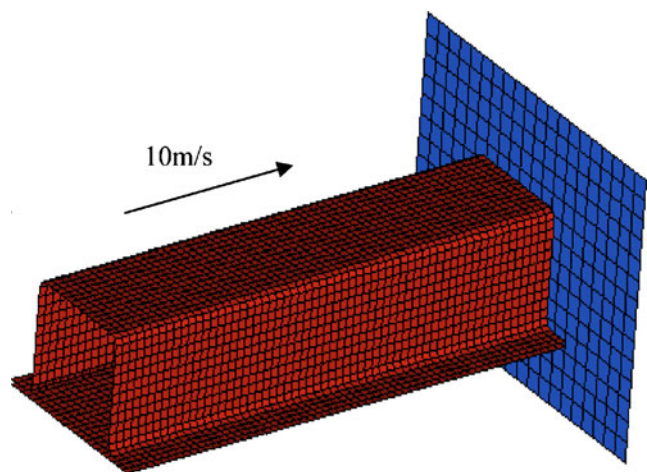


**Fig. 7** FEM mesh of the closed-hat beam impacting a rigid wall

**Table 5** Material properties of the closed-hat beam

Young's modulus $E$ (Mpa)	Poisson's ratio $\nu$	Density $\rho$ (kg/mm <sup>3</sup> )	Yield stress $\sigma_s$ (Mpa)	Tangent Modulus $E_t$ (Mpa)
$2.0 \times 10^5$	0.27	$7.85 \times 10^{-3}$	310	763

optimization problem can be expressed as the following form:

$$\max_{t,R,d} f_e(t, R, d, \sigma_s, E_t)$$

subject to

$$g_f(t, R, d, \sigma_s, E_t) \leq_{mw} [65\text{KN}, 70\text{KN}]$$

$$\sigma_s \in [294.5 \text{ Mpa}, 325.5 \text{ Mpa}],$$

$$E_t \in [724.85 \text{ Mpa}, 801.15 \text{ Mpa}]$$

$$0.5 \text{ mm} \leq t \leq 2.5 \text{ mm}, \quad 1 \text{ mm} \leq R \leq 8 \text{ mm},$$

$$10 \text{ mm} \leq d \leq 60 \text{ mm} \tag{19}$$

where the objective function  $f_e$  and constraint  $g_f$  represent the absorbed energy of the closed-hat beam and the axial impact force respectively, and they are both obtained through the FEM simulation. The maximal generation numbers for outer and inner IP-GA are both specified as 300. The normalization factors  $\phi$  and  $\psi$  are set to 1.9, 2.4 respectively. The allowable errors  $\varepsilon_1 = 0.5$  and  $\varepsilon_2 = 0.15$ . The satisfaction degree level  $\lambda$  and the penalty factor  $\sigma$  are set to 0.8 and 100,000 respectively.

50 initial samples are used to create the approximation models for the uncertain objective and constraint. The result is listed in Table 6. It can be found that the optimal design vector (2.00 mm, 2.75 mm, 34.98 mm)<sup>T</sup> is achieved with the penalty function value  $f_p = 2.32$  after 23 iterations. The interval for energy absorption due to the uncertain parameters is [8.30 kJ, 9.28 kJ], and the interval for average normal impact force is [51.10 kN, 69.74 kN]. Initial samples for objective and constraints can be obtained simultaneously by carrying out the same FEM model, while densified samples during the process should be computed independently. The total number of calling the FEM model is 96.

## 6 Remarks and conclusions

In this paper, a new ANIP method based on a local-densifying method is suggested to promote the efficiency and accuracy of the conventional ANIP method. Under the same or even less computation cost, this new ANIP method has higher accuracy than the conventional ANIP methods. Consequently, high accuracy and low computational cost can be achieved simultaneously. This superiority is more prominent especially for complex problems. Besides, as we only care about the accuracy of approximations in some local regions influencing the solution, more samples are expected to spend there to obtain precise approximations. But on the other hand, if some main characteristics are out of capturing due to the relaxation of approximation quality in the unconcerned regions, the proposed method will reach the local optimum, which is also the main effect of initial sample size, although the local optimal design is often acceptable for practical engineering problems, especially when the systems are complicated.

For large-scale problems, the approximation errors tend to increase exponentially as the dimension increases. The approximation quality can not be guaranteed with a limited sample size. To pursue high accuracy of the approximation for high dimensional problems, a relatively large sample size should be used, which is sometimes unacceptable for practical applications. Nevertheless, a significant improvement of the efficiency and accuracy can still be achieved by the proposed method. Furthermore, if the nonlinearity of the function becomes too high, the local densifying method may have difficulty to identify the key local regions and the algorithm has to make great efforts to revise the approximation models. As a result, this makes this approach quite low efficient. In order to improve the present algorithm, we will consider these abovementioned problems in our future work.

**Table 6** Optimization results of closed-hat beam

Optimal design vector $(t, R, d)$ , mm	$[f^L, f^R]$ , kJ	$[g^L, g^R]$ , kN	Satisfaction degree	$f_p$	NI	Nobj
(2.00, 2.75, 34.98)	[8.30, 9.28]	[51.10, 69.74]	0.88	2.32	23	96

**Acknowledgments** This work is supported by the National Science Fund of China for Distinguished Young Scholars (10725208), the National Science Foundation of China (10802028) and the National 973 Program of China under the Grant No. 2010CB832705.

## References

- Acar E, Solanki K (2009) Improving the accuracy of vehicle crashworthiness response predictions using an ensemble of metamodels. *Int J Crashworthiness* 14(1):49–61
- Au SK, Beck JL (1999) New adaptive importance sampling scheme for reliability calculations. *Struct Saf* 21(2):135–158
- Ben-Haim Y (1994) A non-probabilistic concept of reliability. *Struct Saf* 14(4):227–245
- Ben-Haim Y, Elishakoff I (1990) *Convex models of uncertainties in applied mechanics*. Elsevier Science Publisher, Amsterdam
- Beyer HG, Sendhoff B (2007) Robust optimization—a comprehensive survey. *Comput Methods Appl Mech Eng* 196(33–34):3190–3218
- Chanas S, Kuchta D (1996) Multiobjective programming in optimization of interval objective functions—a generalized approach. *Eur J Oper Res* 94:594–598
- Clarke SM, Griebisch JH, Simpson TW (2005) Analysis of support vector regression for approximation of complex engineering analyses. *J Mech Des* 127(11):1077–1087
- Du X, Chen W (2004) Sequential optimization and reliability assessment method for efficient probabilistic design. *J Mech Des* 126(2):225–233
- Du X, Sudjianto A (2005) Reliability-based design with the mixture of random and interval variables. *J Mech Des* 127(6):1068–1076
- Dyn N, Levin D, Rippa S (1986) Numerical procedures for surface fitting of scattered data by radial basis functions. *J Sci Stat Comp* 7(2):639–659
- Elishakoff I (1995) Discussion on: a non-probabilistic concept of reliability. *Struct Saf* 17(2):195–199
- Elishakoff I, Haftka RT, Fang J (1994) Structural design under bounded uncertainty optimization with anti-optimization. *Comput Struct* 53:1401–1405
- Gunawan S, Azarm S (2005) A feasibility robust optimization method using sensitivity region concept. *J Mech Des* 127(5):858–865
- Ishibuchi H, Tanaka H (1990) Multiobjective programming in optimization of the interval objective function. *Eur J Oper Res* 48:219–225
- Jiang C, Han X, Guan FJ, Li YH (2007a) An uncertain structural optimization method based on nonlinear interval number programming and interval analysis method. *Eng Struct* 29(11):3168–3177
- Jiang C, Han X, Liu GR (2007b) Optimization of structures with uncertain constraints based on convex model and satisfaction degree of interval. *Comput Methods Appl Mech Eng* 196:4791–4800
- Jiang C, Han X, Liu GR (2008) A nonlinear interval number programming method for uncertain optimization problems. *Eur J Oper Res* 188(1):1–13
- Jin Y (2005) A comprehensive survey of fitness approximation in evolutionary computation. *Soft Computing* 9(1):3–12
- Jin R, Chen W, Simpson TW (2001) Comparative studies of meta-modelling techniques under multiple modeling criteria. *Struct Multidisc Optim* 23:1–13
- Jung DH, Lee BC (2002) Development of a simple and efficient method for robust optimization. *Int J Numer Methods Eng* 53(9):2201–2215
- Krishnakumar K (1989) Micro-genetic algorithms for stationary and nonstationary function optimization. In: *SPIE: intelligent control and adaptive systems*, Philadelphia, 289
- Kurtaran H, Eskandarian A, Marzougui D, Bedewi NE (2002) Crashworthiness design optimization using successive response surface approximations. *Comput Mech* 29:409–421
- Lee SH, Chen W (2009) A comparative study of uncertainty propagation methods for black-box-type problems. *Struct Multidisc Optim* 37(3):239–253
- Li G, Li M, Azarm S (2007) Optimizing thermal design of data center cabinets with a new multi-objective genetic algorithm. *Distrib Parallel Database* 21:167–192
- Li G, Li M, Azarm S (2008) A kriging metamodel assisted multi-objective genetic algorithm for design optimization. *J Mech Des* 130:031401
- Liang J, Mourelatos ZP, Tu J (2004) A single loop method for reliability-based design optimization. In: *Proceedings of the ASME DETC'04*, Salt Lake City, UT, September 28 to October 2, paper no. DETC2004-57255
- Liu GR (2003) *Mesh free methods: moving beyond the finite element method*. CRC Press, Boca Raton
- Lombardi M, Haftka R (1998) Anti-optimization technique for structural design under load uncertainties. *Comput Methods Appl Mech Eng* 157(1):19–31
- Luo YJ, Kang Z, Luo Z, Li A (2008) Continuum topology optimization with non-probabilistic reliability constraints based on multi-ellipsoid convex model. *Struct Multidisc Optim* 39:297–310
- Ma LH (2002) Research on method and application of robust optimization for uncertain system. Ph.D. thesis, Zhejiang University China
- Martin JD, Simpson TW (2005) Use of Kriging models to approximate deterministic computer models. *AIAA J* 43(4):853–863
- Möller B, Beer M (2008) Engineering computation under uncertainty—capabilities of non-traditional models. *Comput Struct* 86:1024–1041
- Mullur AA, Messac (2004) A Extended radial basis functions: more flexible and effective metamodeling. In: *Proceedings of the 10th AIAA/ISSMO symposium on multidisciplinary analysis and Optimization*, Albany, NY
- Myers RH, Montgomery DC (2002) *Response surface methodology: process and product optimization using designed experiments*. Wiley, New York
- Parkinson A (1995) Robust mechanical design using engineering models. *J Mech Des* 117(1):48–54
- Penmetsa RC, Grandhi RV (2002) Efficient estimation of structural reliability for problems with uncertain intervals. *Comput Struct* 80(12):1103–1112
- Qiu ZP, Elishakoff I (1998) Anti-optimization of structures with large uncertain-but-non-random parameters via interval analysis. *Comput Methods Appl Mech Eng* 152:361–372
- Queipo NV, Haftka RT, Shyy W, Goel T, Vaidyanathan R, Tucker K (2005) Surrogate-based analysis and optimization. *Prog Aerosp Sci* 41:1–28
- Rao SS, Cao L (2002) Optimum design of mechanical systems involving interval parameters. *J Mech Des* 124(3):465–472
- Sacks J, Welch WJ, Mitchell TJ, Wynn HP (1989) Design and analysis of computer experiments. *Stat Sci* 4(4):409–435
- Smith M (1993) *Neural networks for statistical modeling*. Von Nostrand Reinhold, New York
- Wang HL (2002) Study on optimal design of auto-body structure based on crashworthiness numerical simulation. Ph.D. thesis, Shanghai Jiao Tong University, China
- Wang GG (2003) Adaptive response surface method using inherited Latin hypercube design points. *J Mech Des* 125:210–220

- Wu YT, Millwater HR, Cruse TA (1990) Advanced probabilistic structural-analysis method for implicit performance functions. *AIAA J* 28(9):1663–1669
- Xu YG, Liu GR, Wu ZP (2001) A novel hybrid genetic algorithm using local optimizer based on heuristic pattern move. *Appl Artif Intell* 15:601–631
- Youn BD, Choi KK, Park YH (2003) Hybrid analysis method for reliability-based design optimization. *J Mech Des* 125(2):221–232
- Zhao YG, Ono T (1999) A general procedure for first/second-order reliability method (form/sorm). *Struct Saf* 21(2):95–112